

ON EFFECTIVE NUMERICAL METHODS FOR PHASE-FIELD MODELS

Tao Tang (汤涛)

Abstract

In this article, we overview recent developments of modern computational methods for the approximate solution of phase-field problems. The main difficulty for developing a numerical method for phase field equations is a severe stability restriction on the time step due to nonlinearity and high order differential terms. It is known that the phase field models satisfy a nonlinear stability relationship called gradient stability, usually expressed as a time-decreasing free-energy functional. This property has been used recently to derive numerical schemes that inherit the gradient stability. The first part of the article will discuss implicit-explicit time discretizations which satisfy the energy stability. The second part is to discuss time-adaptive strategies for solving the phase-field problems, which is motivated by the observation that the energy functionals decay with time smoothly except at a few *critical* time levels. The classical operator-splitting method is a useful tool in time discretization. In the final part, we will provide some preliminary results using operator-splitting approach.

1 Introduction

Phase-field models have emerged as a powerful approach for modeling and predicting mesoscale morphological and microstructural evolution in materials. They were originally derived for the microstructure evolution and phase transition, but have been recently extended to many other physical phenomena, such as solid-solid transitions, growth of cancerous tumors, phase separation of block copolymers, dewetting and rupture of thin liquid films and infiltration of water into porous medium. In general, the phase-field models take two distinct values (for instance, $+1$ and -1) in each of the phases, with a smooth change

This work is partially supported by the Special Project on High-Performance Computing of the National Key R&D Program under No. 2016YFB0200604, Hong Kong Research Grants Council CERG grants, National Science Foundation of China, Hong Kong Baptist University FRG grants, and the SUSTech Start-Up Fund.

MSC2010: primary 65M15; secondary 65M70, 35Q35.

Keywords: Phase field equations, energy stability, adaptivity.

between both values in the zone around the interface, which is then diffused with a finite width. Many phenomenological macroscopic coarsening processes are energy driven in the sense that the dynamics is the gradient flow of a certain *energy functional* Kohn [2006].

Two of the phase-field models have attracted much attention: the molecular beam epitaxy (MBE) equation with slope selection

$$(1) \quad u_t = -\delta \Delta^2 u + \nabla \cdot f(\nabla u), \quad x \in \mathbb{R}^d, t \in (0, T],$$

and the Cahn-Hilliard (CH) equation

$$(2) \quad u_t = -\delta \Delta^2 u + \Delta f(u), \quad x \in \mathbb{R}^d, t \in (0, T].$$

In this paper, we consider

$$(3) \quad f(\phi) = \phi|\phi|^2 - \phi$$

for which the two phase-field models (1) and (2) become

$$(4) \quad u_t = -\delta \Delta^2 u + \nabla \cdot (|\nabla u|^2 \nabla u - \nabla u), \quad (x, y) \in \mathbb{R}^d, \quad t \in (0, T],$$

and

$$(5) \quad u_t = -\delta \Delta^2 u + \Delta(u^3 - u), \quad (x, y) \in \mathbb{R}^d, \quad t \in (0, T].$$

In (4), u is a scaled height function of epitaxial growth of thin films in a co-moving frame and the parameter δ is a positive surface diffusion constant. In (5), u represents the concentration of one of the two metallic components of the alloy, and the positive parameter δ represents the interfacial width, which is small compared to the characteristic length of the laboratory scale. An important feature of these two equations is that they can be viewed as the gradient flow of the following energy functionals:

$$(6) \quad E(u) = \int_{\Omega} \left[\frac{\delta}{2} |\Delta u|^2 + \frac{1}{4} (|\nabla u|^2 - 1)^2 \right] dx$$

for the MBE equation and

$$(7) \quad E(u) = \int_{\Omega} \left[\frac{\delta}{2} |\nabla u|^2 + \frac{1}{4} (|u|^2 - 1)^2 \right] dx$$

for the CH one. It is well known that both energy functionals decay in time

$$(8) \quad E(u(t)) \leq E(u(s)), \quad \forall t \geq s.$$

In this paper, we will review some recent works developing highly efficient numerical methods for phase field models. The main stability criteria is the energy decay principle (8). Among the time discretizations based on (8), Eyre's [Eyre \[1993\]](#) convex splitting scheme should be specially mentioned. It is a first-order accurate unconditionally stable time-stepping scheme for gradient flows, which can be either linear or nonlinear depending on the ways of splitting. In particular, it has served as inspiration for many other time integration schemes in recent years, see, e.g., [Feng, Tang, and J. Yang \[2015\]](#), [Qiao and S. Sun \[2014\]](#), [Shen, C. Wang, X. Wang, and Wise \[2012\]](#), and [Shen, J. Xu, and J. Yang \[2017\]](#). Other significant works for higher order stable schemes for the phase field models can be found in [Gomez and Hughes \[2011\]](#), [Qiao, Z.-Z. Sun, and Z. Zhang \[2015\]](#), [Shen, C. Wang, X. Wang, and Wise \[2012\]](#), [Wise, C. Wang, and Lowengrub \[2009\]](#), [Xia, Y. Xu, and Shu \[2009\]](#), and [van der Zee, Oden, Prud'homme, and Hawkins-Daarud \[2011\]](#).

2 Time stabilization by adding consistent terms

Since explicit schemes usually suffer from severe stability restrictions caused by the presence of high-order derivative terms and do not obey the energy decay property, semi-implicit schemes are widely used. It is known that explicit schemes usually suffer severe time step restrictions and generally do not obey energy conservation. To enforce the energy decay property and increase the time step, a good alternative is to use implicit-explicit (semi-implicit) schemes in which the linear part is treated implicitly (such as backward differentiation in time) and the nonlinear part is evaluated explicitly. For example, in [L.Q. Chen \[1998\]](#) Chen and Shen considered the semi-implicit Fourier-spectral scheme for (5) (set $\delta = 1$)

$$(1) \quad \frac{\widehat{u}^{n+1}(k) - \widehat{u}^n(k)}{\Delta t} = -|k|^4 \widehat{u}^{n+1}(k) - |k|^2 \widehat{f}(\widehat{u}^n)(k),$$

where \widehat{u}^n denotes the Fourier coefficient of u at time step t_n . On the other hand, the semi-implicit schemes can generate large truncation errors. As a result smaller time steps are usually required to guarantee accuracy and (energy) stability. To resolve this issue, a class of large time-stepping methods were proposed and analyzed in [Feng, Tang, and J. Yang \[2013\]](#), [He, Liu, and Tang \[2007\]](#), [Shen and X. Yang \[2010\]](#), [C. Xu and Tang \[2006\]](#), and [Zhu, Chen, Shen, and Tikare \[1999\]](#). The basic idea is to add an $O(\Delta t)$ stabilizing term to the numerical scheme to alleviate the time step constraint whilst keeping energy stability.

The choice of the $O(\Delta t)$ term is quite flexible. For example, in [Zhu, Chen, Shen, and Tikare \[1999\]](#) the authors considered the Fourier spectral approximation of the modified Cahn-Hilliard-Cook equation

$$(2) \quad \partial_t C = \nabla \cdot ((1 - aC^2)\nabla(C^3 - C - \kappa\nabla^2 C)).$$

The explicit Fourier spectral scheme is (see equation (16) therein)

$$(3) \quad \frac{\widehat{C}^{n+1}(k, t) - \widehat{C}^n(k, t)}{\Delta t} = ik \cdot \{(1 - aC^2)[ik'(\{-C + C^3\}_k^n + \kappa|k'|^2\widehat{C}^n(k', t))]\}_k.$$

The time step for the above scheme has a severe constraint

$$(4) \quad \Delta t \cdot \kappa \cdot K^4 \leq 1,$$

where K is the number of Fourier modes in each coordinate direction. To increase the allowable time step, it is proposed in [Zhu, Chen, Shen, and Tikare \[ibid.\]](#) to add a term $-Ak^4(\widehat{C}^{n+1} - \widehat{C}^n)$ to the RHS of (3). Note that on the real side, this term corresponds to a fourth order dissipation, i.e.

$$-A\Delta^2(C^{n+1} - C^n)$$

which roughly is of order $O(\Delta t)$.

In [He, Liu, and Tang \[2007\]](#), a stabilized semi-implicit scheme was considered for the CH model, with the use of an order $O(\Delta t)$ stabilization term

$$A\Delta(u^{n+1} - u^n).$$

Under a condition on A of the form:

$$(5) \quad A \geq \max_{x \in \Omega} \left\{ \frac{1}{2}|u^n(x)|^2 + \frac{1}{4}|u^{n+1}(x) + u^n(x)|^2 \right\} - \frac{1}{2}, \quad \forall n \geq 0,$$

one can obtain energy stability (8). Note that the condition (5) depends nonlinearly on the numerical solution. In other words, it implicitly uses the L^∞ -bound assumption on u^n in order to make A a controllable constant.

In 2010, Shen and Yang proved energy stability of semi-implicit schemes for the Allen-Cahn and the CH equations with truncated nonlinear term. More precisely it is assumed

that

$$(6) \quad \max_{u \in \mathbb{R}} |f'(u)| \leq L \square \square$$

which is what we referred to as the Lipschitz assumption on the nonlinearity in the abstract.

In 2011, Bertozzi et al. considered a nonlinear diffusion model of the form

$$\partial_t u = -\nabla \cdot (f(u) \nabla \Delta u) + \nabla \cdot (g(u) \nabla u),$$

where $g(u) = f(u)\phi'(u)$, and f, ϕ are given smooth functions. In addition f is assumed to be non-negative. The numerical scheme considered in Bertozzi, Ju, and Lu [2011] takes the form

$$(7) \quad \frac{u^{n+1} - u^n}{\Delta t} = -A\Delta^2(u^{n+1} - u^n) - \nabla \cdot (f(u^n) \nabla \Delta u^n) + \nabla \cdot (g(u^n) \nabla u^n),$$

where $A > 0$ is a parameter to be taken large. One should note the striking similarity between this scheme and the one introduced in Zhu, Chen, Shen, and Tikare [1999]. In particular in both papers the biharmonic stabilization of the form $-A\Delta^2(u^{n+1} - u^n)$ was used. The analysis in Bertozzi, Ju, and Lu [2011] is carried out under the additional assumption that

$$(8) \quad \sup_n \|f(u^n)\|_\infty \leq A < \infty.$$

This is reminiscent of the L^∞ bound on u^n .

Roughly speaking, all prior analytical developments are conditional in the sense that either one makes a Lipschitz assumption on the nonlinearity, or one assumes certain a priori L^∞ bounds on the numerical solution. It is very desirable to *remove these technical restrictions* and establish a more reasonable stability theory.

In D. Li, Qiao, and Tang [2016], this problem is settled for the spectral Galerkin case. More precisely, the authors of D. Li, Qiao, and Tang [ibid.] considered a stabilized semi-implicit scheme introduced in He, Liu, and Tang [2007] following the earlier work C. Xu and Tang [2006]. It takes the form

$$(9) \quad \begin{cases} \frac{u^{n+1} - u^n}{\Delta t} = -\delta\Delta^2 u^{n+1} + A\Delta(u^{n+1} - u^n) + \Delta \Pi_N(f(u^n)), & n \geq 0, \\ u^0 = \Pi_N u_0. \end{cases}$$

where $A > 0$ is the coefficient for the $O(\Delta t)$ regularization term. For each integer $N \geq 2$, define

$$X_N = \text{span} \left\{ \cos(k \cdot x), \sin(k \cdot x) : k = (k_1, k_2) \in \mathbb{Z}^2, |k|_\infty = \max\{|k_1|, |k_2|\} \leq N \right\}.$$

Note that the space X_N includes the constant function (by taking $k = 0$). The L^2 projection operator $\Pi_N : L^2(\Omega) \rightarrow X_N$ is defined by

$$(10) \quad (\Pi_N u - u, \phi) = 0, \quad \forall \phi \in X_N,$$

where (\cdot, \cdot) denotes the usual L^2 inner product on Ω . In yet other words, the operator Π_N is simply the truncation of Fourier modes of L^2 functions to $|k|_\infty \leq N$. Since $\Pi_N u_0 \in X_N$, by induction it is easy to check that $u^n \in X_N$ for all $n \geq 0$.

Theorem 2.1 (Unconditional energy stability for 2D CH). *Consider (9) with $\delta > 0$ and assume $u_0 \in H^2(\Omega)$ with mean zero. Denote $E_0 = E(u_0)$ the initial energy. There exists a constant $\beta_c > 0$ depending only on E_0 such that if*

$$(11) \quad A \geq \beta \cdot \left(\|u_0\|_{H^2}^2 + \delta^{-1} |\log \delta|^2 + 1 \right), \quad \beta \geq \beta_c,$$

then

$$E(u^{n+1}) \leq E(u^n), \quad \forall n \geq 0,$$

where E is defined by (7). Furthermore, let $u_0 \in H^s$, $s \geq 4$ with mean zero. Let $u(t)$ be the solution to (5) with initial data u_0 . Let u^n be defined according to (9) with initial data $\Pi_N u_0$. If A satisfies (11), then

$$\|u(t_m) - u^m\|_2 \leq A \cdot e^{C_1 t_m} \cdot C_2 \cdot (N^{-s} + \Delta t).$$

where $t_m = m\Delta t$, $C_1 > 0$ depends only on (u_0, δ) , $C_2 > 0$ depends on (u_0, δ, s) .

There is an analogue of [Theorem 2.1](#) for the MBE [Equation \(4\)](#). Consider the following semi-implicit scheme for MBE (4):

$$(12) \quad \begin{cases} \frac{u^{n+1} - u^n}{\tau} = -\delta \Delta^2 u^{n+1} + A \Delta (u^{n+1} - u^n) + \Pi_N \nabla \cdot (g(\nabla u^n)), & n \geq 0, \\ u^0 = \Pi_N u_0. \end{cases}$$

This scheme was introduced and analyzed in [C. Xu and Tang \[2006\]](#) (see also [Qiao, Z. Zhang, and Tang \[2011\]](#)). The authors of [C. Xu and Tang \[2006\]](#) first introduced the

stabilized $O(\Delta t)$ term of the form $A\Delta(u^{n+1} - u^n)$ as given in (12), and provided an energy stability analysis based on the assumption that A depends implicitly on the L^∞ bound on the numerical solution u^n . Note that the result in D. Li, Qiao, and Tang [2016] provide a clean description on the size of the constant A , in the sense that A is independent of the L^∞ bound on the numerical solution. The energy-supercritical three-dimensional case is analysed in D. Li and Qiao [2017b] by exploiting discrete smoothing estimates.

Note that above results are restricted to the first-order time discretization. On the other hand, D. Li and Qiao [2017a] introduced recently several novel stabilization techniques for second-order schemes. Quite surprisingly, it is found that depending on the form of numerical discretization (such as $f(2u^n - u^{n-1})$ v.s. $2f(u^n) - f(u^{n-1})$) the corresponding scheme can have conditional stability or unconditional stability with the stabilization parameter depending only on initial data and the diffusion coefficient. Developing upon the second-order scheme in D. Li and Qiao [ibid.], Song and Shu [2017] constructed a new unconditionally stable second-order implicit–explicit local discontinuous Galerkin Method for the Cahn–Hilliard Equation.

3 Time stepping with p -adaptivity

As the governing equations (4) and (5) involve the perturbed (i.e., the coefficient $\delta \ll 1$) biharmonic operators and strong nonlinearities, it is very difficult to design efficient time discretization strategy which can resolve dynamics and steady state of the corresponding phase field models. Moreover, nonlinear energy stability which is intrinsic to the phase field models (see, e.g., Figure 1) is also a challenging issue for numerical approximations. Numerical evidences show that violating the energy stability may lead to non-physical oscillations. Consequently, a satisfactory numerical strategy needs to balance solution accuracy, efficiency and nonlinear stability.

Below we will briefly outline the motivation of this section. Our numerical evidences show that the lower order time discretizations may require very small time stepsizes in order to resolve the short time dynamics of the phase field problems. Figure 2 gives a typical example which gives energy evolutions for the Cahn-Hilliard Equation (5) with $\Delta t = 1/1000, 1/100, 1/50$. It is observed that a time step smaller than 10^{-2} is needed in order to obtain accurate solutions.

For improvement, one quick idea is to use higher order time discretization. However, there has few higher order energy-stable schemes, particularly for order 3 or higher. Our idea is to use the so-called spectral deferred correction (SDC) method which was first introduced to solve initial value ordinary differential equations (ODEs) by Dutt, Greengard, and Rokhlin [2000]. The key idea of the SDC method is to first convert the original ODEs into the corresponding Picard equation and then apply a deferred correction procedure

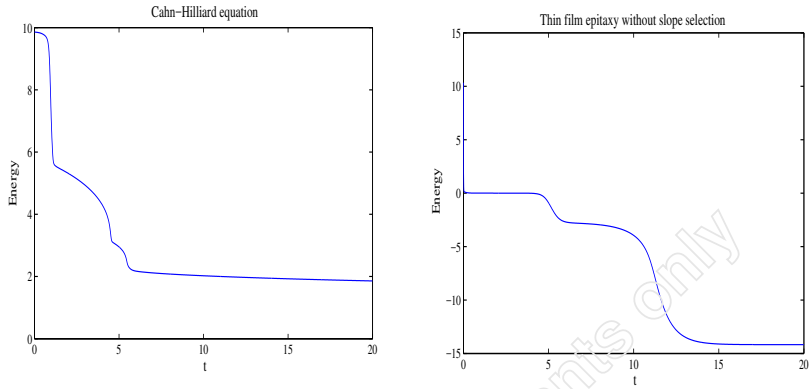


Figure 1: Illustrative energy curves for the three different models.

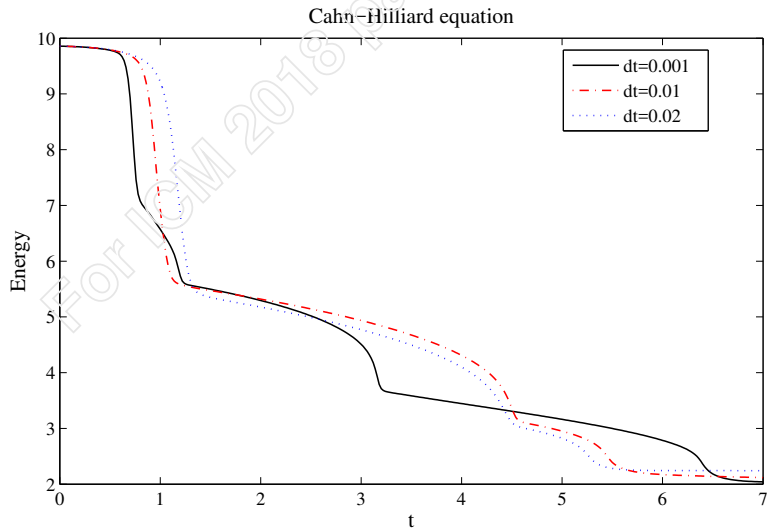


Figure 2: A typical example for the energy dependent on time steps for the Cahn-Hilliard equation.

in the integral formulation, aiming to achieve higher order accuracy in an *iterative* way.

The reasons for us to employ the SDC method are the following: iteration loops can improve the formal accuracy in a flexible and simple way; the SDC method was designed to handle stiff systems which are the case of our perturbed singularly nonlinear equations; and the flexibility of the order enhancement is useful for our local adaptive strategy to be described later. On the other hand, although the SDC method can solve the short-time dynamics very well (e.g., a 5th-order time discretization can fix the problem in Figure 2 with $\Delta t = 1/20$), unfortunately, a higher order time discretization may yield numerical instability as the nonlinear stability can not be guaranteed for higher order time discretizations. A typical example is given in Figure 3, which solves the same example as in Figure 2 but with an 3rd order SDC method (i.e. $Np = 2$ in the figure) and an 5th-order SDC method (i.e. $Np = 4$). It is observed that the discrete energies blow up before $T = 30$.

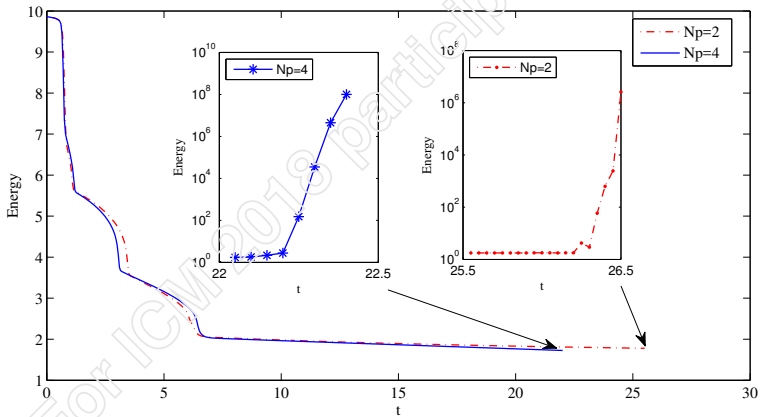


Figure 3: A typical energy blow-up with 3rd (right) or a 5th (left) order time discretization for the Cahn-Hilliard equation.

Note that the problem in Figs. 2 and 3 is partially due to the use of the central-difference approaches in space approximation (see Feng, Tang, and J. Yang [2015]). A more elegant approach using discontinuous Galerkin (DG) method together with SDC methods. Stable and accurate numerical results have been obtained in Guo and Y. Xu [2016] and Guo, Xia, and Y. Xu [2017]. On the other hand, for simple central-difference approaches in space, we can use a hybrid p -adaptive method which chooses appropriate order of accuracy at each time level. It is seen from the energy curves in Figure 1 that first-order methods should be good enough in most of time regimes, but in some critical stages with rapid

energy change appropriate adaptive strategies must be used. Some p -adaptive details will be reported and the relevant numerical results will be presented in this section.

3.1 Convex splitting methods. An important class of time discretization is the convex splitting method originally proposed by Eyre [1993], see also improved version of Shen, J. Xu, and J. Yang [2017] and Shen, C. Wang, X. Wang, and Wise [2012], which can produce *unconditional* energy stability (in the sense that the stability is irrelevant with the choice of the time steps). If we can express the free energy as the difference of two convex functional, namely $E = E_c - E_e$, where both E_c and E_e are convex about u , then we may use the concept of convex splitting due to Eyre [1993] to obtain highly stable numerical schemes.

Below we will demonstrate the convex splitting by considering the Cahn-Hilliard Equation (5). Using the splitting form

$$(1) \quad E_c(u) = \int_{\Omega} \left(\frac{\delta}{2} |\nabla u|^2 + \frac{\beta}{2} u^2 \right) dx, \quad E_e(u) = \int_{\Omega} \left(\frac{\beta}{2} u^2 - F(u) \right) dx,$$

where $F = (|u|^2 - 1)^2/4$, and the corresponding semi-discrete scheme to the Cahn-Hilliard Equation (5) is

$$(2) \quad \frac{u^{n+1} - u^n}{\Delta t} = \Delta \left(\frac{\delta E_c(u^{n+1})}{\delta u} - \frac{\delta E_e(u^n)}{\delta u} \right) \\ = -\epsilon^2 \Delta^2 u^{n+1} + \beta \Delta u^{n+1} - \beta \Delta u^n + \Delta f(u^n).$$

It can be proven (see, e.g., Feng, Tang, and J. Yang [2015]) that if the constant β is sufficiently large then the semi-discrete scheme (2) is unconditionally energy stable, i.e., $E(u^{n+1}) \leq E(u^n)$, where the energy E is defined by (7). Similarly, for the MBE model (4), using the convex splitting

$$(3) \quad E_c(u) = \int_{\Omega} \left(\frac{\epsilon^2}{2} |\Delta u|^2 + \frac{\beta}{2} |\nabla u|^2 \right) dx, \quad E_e(u) = \int_{\Omega} \left(\frac{\beta}{2} |\nabla u|^2 - F(\nabla u) \right) dx,$$

gives the corresponding semi-discrete scheme

$$(4) \quad \frac{u^{n+1} - u^n}{\Delta t} = - \left(\frac{\delta E_c(u^{n+1})}{\delta u} - \frac{\delta E_e(u^n)}{\delta u} \right) \\ = -\epsilon^2 \Delta^2 u^{n+1} + \beta \Delta u^{n+1} - \beta \Delta u^n + \nabla \cdot f(\nabla u^n).$$

In practical computations, for both (4) and (5) with $f(u)$ of the form (3), $\beta = 1$ can guarantee the energy stability for (4), and $\beta = 2$ can guarantee the energy stability for (2).

3.2 Spectral deferred correction method. Assume the time interval $[0, T]$ into N non-overlapping intervals $0 = t_0 < t_1 < \dots < t_N = T$. Let $\Delta t_n = t_{n+1} - t_n$ and u_n denotes the numerical solution of $u(t_n)$, with $u_0 = u(t_0)$. Based on the convex splitting schemes presented in the above subsection, our convex splitting scheme can be written in the following form

$$(5) \quad u^{n+1} = u^n + \Delta t_n (F_E(u^n) + F_I(u^{n+1}))$$

for convenience, where F_N represents the explicit part and F_I represents the implicit part.

The SDC method is a one step, multi-stage method. Denoting the $p + 1$ Legendre-Guass-Radau IIa nodes (cf. [Shen, Tang, and L.-L. Wang \[2011\]](#)) on $[-1, 1]$ by $-1 = r_0 < r_1 < \dots < r_{p-1} < r_p = 1$ and letting

$$t_{n,i} = \frac{t_{n+1} - t_n}{2} r_i + \frac{t_{n+1} + t_n}{2}, \quad i = 0, 1, \dots, p,$$

we obtain the spectral nodes on interval $[t_n, t_{n+1}]$ of the form $t_n = t_{n,0} < t_{n,1} < \dots < t_{n,p-1} < t_{n,p} = t_{n+1}$. Then the interval $[t_n, t_{n+1}]$ is divided into p subintervals. Let $\Delta t_{n,m} = t_{n,m+1} - t_{n,m}$ and $u_{n,m}^k$ denotes the k^{th} order approximation to $u(t_{n,m})$.

Note that we do the SDC procedure in every interval $[t_n, t_{n+1}]$. Given u_n , we wish to approximate u_{n+1} . Let $u_{n,0}^1 = u_n$. We first compute a first order accurate approximate solution u^1 at the nodes $\{t_{n,m}\}_{m=1}^p$:

$$(6) \quad u_{n,m+1}^1 = u_{n,m}^1 + \Delta t_{n,m} (F_E(t_{n,m}, u_{n,m}^1) + F_I(t_{n,m+1}, u_{n,m+1}^1)).$$

We then do the successive corrections. For each $1 \leq k \leq K$, let $u_{n,0}^{k+1} = u_n$. For $m = 0, \dots, p-1$, we use

$$(7) \quad u_{n,m+1}^{k+1} = u_{n,m}^{k+1} + \Delta t_{n,m} (F_E(t_{n,m}, u_{n,m}^{k+1}) - F_E(t_{n,m}, u_{n,m}^k) + F_I(t_{n,m+1}, u_{n,m+1}^{k+1}) - F_I(t_{n,m+1}, u_{n,m+1}^k)) + I_m^{m+1}(F_E(t, u^k) + F_I(t, u^k)),$$

where the last part is the integral of the p -th degree interpolating polynomial on the $p + 1$ points

$$(t_{n,m}, F_E(t_{n,m}, u_{n,m}^k) + F_I(t_{n,m}, u_{n,m}^k))_{m=0}^p$$

over the subinterval $[t_{n,m}, t_{n,m+1}]$, which is the numerical quadrature approximation of

$$\int_{t_{n,m}}^{t_{n,m+1}} (F_E(\tau, u(\tau)) + F_I(\tau, u(\tau))) d\tau.$$

The above procedure leads to $u_{n+1} = u_{n,p}^{K+1}$.

For more details of the SDC method, we refer the readers to [Dutt, Greengard, and Rokhlin \[2000\]](#) and [Minion \[2003\]](#) and the recent work [Guo and Y. Xu \[2016\]](#) and [Tang, Xie, and Yin \[2013\]](#).

3.3 Efficiency enhancement with p -adaptivity. It is known that the convex splitting method can preserve the energy stability but accuracy may not be satisfactory. Although using SDC may enhance accuracy, the SDC corrections may cause blow-up as demonstrated in Fig. 3. It remains to balance the accuracy and stability. To this end, an adaptive strategy adjusting the correction number was proposed in [Feng, Tang, and J. Yang \[2015\]](#) based on the discrete energies $E_h(u^n)$ and $E_h(u^{n-1})$:

(8)

$$Np = \min\{Nmax, \max\{0, Nmax + \text{fix}[\log_\eta(|E_h(u^n) - E_h(u^{n-1})| + \eta^{-(Nmax+1)})]\}\},$$

where η is a positive constant, $Nmax$ is the maximum number of corrections and $\text{fix}[\cdot]$ represents the integer part of a number. Below we will explain the motivation of using (8) to predict Np . It is clear that more corrections are needed in the region where the energy decays fast. More specifically, the relationship between Np and the energy change is given as following:

$$(9) \quad Np = \begin{cases} 0, & \text{if } |E_h(u^n) - E_h(u^{n-1})| < \eta^{-Nmax} \\ k, & \text{if } \eta^{-Nmax+k} \leq |E_h(u^n) - E_h(u^{n-1})| < \eta^{-Nmax+k+1} \\ Nmax, & \text{if } |E_h(u^n) - E_h(u^{n-1})| \geq \eta^{-1} \end{cases},$$

where $Nmax$ is upper bounded by $2p - 1$ as the accuracy order of the interpolation on the $p + 1$ Gauss-Radau nodes is $2p$ and the parameter η can be fixed as 3 or 5.

Note that the energy decreasing property motivates us to use the energy difference at t_{n-1} and t_n for choosing the number of corrections. Firstly, as observed from the energy curves in [Figure 1](#), the energy variation in most time regimes is very small, so $Np = 0$ should be chosen in most of the time intervals. This implies that only first order SDC method is used, which guarantees the energy stability in general. Secondly, in the transition regime, the energy variation is between η^{-Nmax} and η^{-1} , which indicates some variable value of Np is used based on the size of the energy variation. Thirdly, if the energy variation exceeds η^{-1} , then the maximum number of correction should be used. In the later two cases, the energy decreasing property may not be preserved locally. However, as the total number of the intervals relevant to the last two cases is very small, it is expected that the overall energy stability can be preserved well. In other words, the choice of (9) seems very useful to balance the accuracy and overall energy stability.

Example 3.1. We will use the adaptive SDC scheme for the Cahn-Hilliard Equation (5) with initial condition $u_0(x, y) = 0.05 \sin x \sin y + 0.001$, $0 \leq x, y \leq 2\pi$, and the periodic boundary condition. The parameter δ is chosen as 0.01.

The mesh grid in space is fixed as 400×400 . We take the numerical solutions with small uniform time step $dt = 0.001$ as the “reference” solution. We take $p = 4$ in the SDC method, and $\beta = 1$ in (2), $\eta = 5$, $Nmax = 5$ in (9) and set $Np = Nmax$ at the first step.

In Figure 4, the numerical results using adaptive SDC scheme with $dt = 0.04$ produce graphically indistinguishable energy curve as that for un-adaptive $dt = 0.001$ results. On the other hand, the energy curve with un-adaptive $dt = 0.04$ is quite far from the reference energy curve, especially before $T = 10$, which can be seen in the locally magnified energy curves from $T = 2$ to 8.

The CPU time comparison is presented in Figure 5, where it is seen that our adaptive SDC scheme consumes more CPU time at beginning as more corrections are needed to capture the fast dynamical evolution. However, the adaptive SDC scheme can enhance the efficiency significantly in the long time computation. The numerical solutions at different time levels are presented in Figure 6, where it is observed that the solution dynamics can be captured correctly with larger time steps when adaptive strategy is employed.

4 Operator splitting method

Following the approach in Chertock, Kurganov, and Petrova [2009], we split Eq. (4) into the nonlinear part

$$(1) \quad u_t = \nabla \cdot (|\nabla u|^2 \nabla u),$$

and linear part

$$(2) \quad u_t = -\Delta u - \delta \Delta^2 u.$$

We denote by \mathcal{S}_n the exact solution operator associated with (1) and by $\mathcal{S}_\mathcal{L}$ the exact solution operator associated with (2). Notice that the corresponding energy functionals,

$$(3) \quad E_n(u) = \frac{1}{4} \int_{\Omega} |\nabla u|^4 dx dy,$$

$$(4) \quad E_\mathcal{L}(u) = \int_{\Omega} \left(\frac{\delta}{2} |\Delta u|^2 - \frac{1}{2} |\nabla u|^2 + \frac{1}{4} \right) dx dy$$

decay. Then, introducing a (small) splitting step Δt , the solution of the original equation (4) (which is assumed to be available at time t) is evolved using the Strang splitting method, one step of which can be written as

$$u(x, y, t + \Delta t) = \mathfrak{S}_{\mathcal{L}}(\Delta t/2)\mathfrak{S}_{\mathfrak{n}}(\Delta t)\mathfrak{S}_{\mathcal{L}}(\Delta t/2)u(x, y, t).$$

A similar splitting approach is applied to equation (5), for which the linear part is still (2) and the nonlinear one is

$$(5) \quad u_t = \Delta(u^3).$$

As in the case of the MBE equation, the corresponding energy functionals,

$$(6) \quad E_{\mathfrak{n}}(u) = \frac{1}{4} \int_{\Omega} u^4 dx dy,$$

$$(7) \quad E_{\mathcal{L}}(u) = \int_{\Omega} \left(\frac{\delta}{2} |\nabla u|^2 - \frac{i}{2} u^2 + \frac{1}{4} \right) dx dy$$

decay. We stress that even though the linear parts of equations (4) and (5) are the same, the functionals (4) and (7) are different since they are associated with the corresponding parts of the energy functionals (6) and (7).

In order to implement the splitting method, the exact solution operators $\mathfrak{S}_{\mathfrak{n}}$ and $\mathfrak{S}_{\mathcal{L}}$ have to be replaced by their numerical approximations. Note that one of the main advantages of the operator splitting technique is the fact that the nonlinear, (1) and (5), and linear, (2), subproblems, which are of different nature, can be solved numerically by different methods. First, using the method of lines, (1) and (5) can be reduced to systems of ODEs, which can be efficiently and accurately integrated by large stability domain explicit ODE solvers [Abdulle \[2002\]](#). Second, since (2) is linear, one can solve it (practically) exactly using, for example, the pseudo-spectral method. This way, no stability restrictions on solving (2) are imposed.

4.1 Finite-Difference Methods for (1) and (5). In this section, we propose efficient explicit finite-difference methods for the degenerate parabolic equations (1) and (5). These methods are based on the semi-discretization of (1) and (5) followed by the use of an efficient and accurate ODE solver. The ODE solver will be utilized to evolve the solutions of (1) and (5) from time t to $t + \Delta t$. We note that in a general case the time-steps of the ODE solver denoted by Δt_{ODE} will be smaller than the splitting step Δt so that the approximation of $\mathfrak{S}_{\mathfrak{n}}(\Delta t)$ will typically require several Δt_{ODE} steps.

We first design $2m$ th-order centered-difference schemes for the 1-D version of (1):

$$(8) \quad u_t = (u_x^3)_x, \quad x \in [0, L], \quad t \in (0, T].$$

We consider a uniform grid with nodes x_j , such that $x_{j+1} - x_j = \Delta x$, $\forall j$, and introduce the following $2m$ th-order discrete approximation of the $\frac{\partial}{\partial x}$ operator:

$$(9) \quad (\psi_x)_j := \sum_{p=-m}^m \alpha_p \psi_{j+p} = \psi_x(x_j) + \mathcal{O}((\Delta x)^{2m}).$$

For example, when $m = 2$, we obtain a fourth-order centered-difference approximation by taking

$$\alpha_1 = -\alpha_{-1} = \frac{2}{3\Delta x}, \quad \alpha_2 = -\alpha_{-2} = -\frac{1}{12\Delta x}.$$

Equipped with the above approximation of spatial derivatives, we discretize equation (8) using the method of lines as follows:

$$(10) \quad \frac{du_j}{dt}(t) = \sum_{p=-m}^m \alpha_p H_{j+p}(t) =: F_j(t),$$

where $u_j(t)$ denotes the computed point value of the solution at (x_j, t) , and

$$(11) \quad H_j(t) := (u_x)_j^3(t) \quad \text{with} \quad (u_x)_j(t) := \sum_{p=-m}^m \alpha_p u_{j+p}(t).$$

Note that the above quantities depend on t , but for the sake of brevity we will suppress this dependence from now on.

It is proven in [Cheng, Kurganov, Qu, and Tang \[2015\]](#) that the semi-discrete schemes (10)-(11) satisfy the following energy decay property:

$$\frac{d}{dt} E_{\mathbf{n}}^{\Delta} \leq 0,$$

where $E_{\mathbf{n}}^{\Delta}$ is a 1-D discrete version of the energy functional (3): $E_{\mathbf{n}}^{\Delta} := \frac{1}{4} \sum_j (u_x)_j^4 \Delta x$.

We now consider the finite-difference schemes for $u_t = \nabla \cdot (|\nabla u|^2 \nabla u)$, i.e., (1). We consider a uniform grid with nodes (x_j, y_k) , such that $x_{j+1} - x_j = \Delta x$, $\forall j$, $y_{k+1} - y_k = \Delta y$, $\forall k$, and introduce the following $2m$ th-order discrete approximation of the $\frac{\partial}{\partial x}$ and $\frac{\partial}{\partial y}$

operators:

$$(12) \quad \begin{aligned} (\psi_x)_{j,k} &:= \sum_{p=-m}^m \alpha_p \psi_{j+p,k} = \psi_x(x_j, y_k) + \mathcal{O}((\Delta x)^{2m}), \\ (\psi_y)_{j,k} &:= \sum_{p=-m}^m \beta_p \psi_{j,k+p} = \psi_y(x_j, y_k) + \mathcal{O}((\Delta y)^{2m}). \end{aligned}$$

For example, when $m = 2$, we obtain a fourth-order centered-difference approximation by taking

$$\alpha_1 = -\alpha_{-1} = \frac{2}{3\Delta x}, \quad \alpha_2 = -\alpha_{-2} = -\frac{1}{12\Delta x}, \quad \beta_1 = -\beta_{-1} = \frac{2}{3\Delta y}, \quad \beta_2 = -\beta_{-2} = -\frac{1}{12\Delta y}$$

Equipped with the above approximation of spacial derivatives, $2m$ th-order semi-discrete finite-difference schemes for (1) read:

$$(13) \quad \frac{du_{j,k}}{dt} = \sum_{p=-m}^m \alpha_p H_{j+p,k}^x + \sum_{p=-m}^m \beta_p H_{j,k+p}^y =: F_{j,k},$$

where

$$(14) \quad H_{j,k}^x := (u_x)_{j,k}^3 + (u_y)_{j,k}^2 (u_x)_{j,k} \quad \text{and} \quad H_{j,k}^y := (u_y)_{j,k}^3 + (u_x)_{j,k}^2 (u_y)_{j,k}$$

with

$$(15) \quad (u_x)_{j,k} := \sum_{p=-m}^m \alpha_p u_{j+p,k} \quad \text{and} \quad (u_y)_{j,k} := \sum_{p=-m}^m \beta_p u_{j,k+p}.$$

It is shown in [Cheng, Kurganov, Qu, and Tang \[2015\]](#) that the semi-discrete schemes (13)–(15) satisfy the following energy decay property:

$$\frac{d}{dt} E_{\mathbf{n}}^{\Delta} \leq 0,$$

where $E_{\mathbf{n}}^{\Delta}$ is a 2-D discrete version of the energy functional (3): $E_{\mathbf{n}}^{\Delta} := \frac{1}{4} \sum_j |\nabla_h u_{j,k}|^4 \Delta x \Delta y$ with $\nabla_h u_{j,k} := ((u_x)_{j,k}, (u_y)_{j,k})^T$.

We now design semi-discrete finite-difference schemes for $u_t = \Delta(u^3)$, i.e., (5). We use the same grids and the same $2m$ th-order discrete approximation of the $\frac{\partial}{\partial x}$ and $\frac{\partial}{\partial y}$

operators as above. Then, $2m$ th-order semi-discrete finite-difference schemes for (5) read:

$$(16) \quad \frac{du_{j,k}}{dt} = \sum_{p=-m}^m \alpha_p H_{j+p,k}^x + \sum_{p=-m}^m \beta_p H_{j,k+p}^y =: F_{j,k},$$

where

$$(17) \quad H_{j,k}^x := \sum_{p=-m}^m \alpha_p u_{j+p,k}^3 \quad \text{and} \quad H_{j,k}^y := \sum_{p=-m}^m \beta_p u_{j,k+p}^3.$$

It can be shown that the semi-discrete schemes (16)-(17) satisfy the following energy decay property:

$$\frac{d}{dt} E_{\mathbf{n}}^{\Delta} \leq 0,$$

where $E_{\mathbf{n}}^{\Delta}$ is a 2-D discrete version of the energy functional (6): $E_{\mathbf{n}}^{\Delta} := \frac{1}{4} \sum_j u_{j,k}^4 \Delta x \Delta y$.

4.2 Large Stability Domain Explicit ODE Solver. The ODE systems (10), (13) and (16) have to be solved numerically. Recall that explicit ODE solvers typically require time-steps to be $\Delta t_{\text{ODE}} \sim (\Delta x)^2$, while implicit ODE solvers can be made unconditionally stable. However, the accuracy requirements would limit time-step size and since a large nonlinear algebraic system of equations has to be solved at each time-step, implicit methods may not be efficient. Here, we apply the explicit third-order large stability domain Runge-Kutta method, developed in Medovikov [1998] and Medovikov [n.d.], which allow one to use much larger time-steps compared with the standard explicit Runge-Kutta methods. In practice, when the problem is not too stiff as in the case of ODEs arising in finite-difference approximation of parabolic PDEs, these methods preserve all the advantages of explicit methods and are typically more efficient than implicit methods (see Abdulle [2002], Medovikov [1998], and Verwer, Sommeijer, and Hundsdorfer [2004] for details). We have implemented the code DUMKA3 Medovikov [n.d.], which incorporates the embedded formulas that permit an efficient stepsize control. The efficiency of DUMKA3 is further improved when the user provides an upper bound on the time-step stability restriction for the forward Euler method. Assume that the system of ODEs (10)-(11) is numerically integrated by the forward Euler method from time t to $t + \Delta t_{\text{FE}}$ and that the following CFL condition holds:

$$(18) \quad \Delta t_{\text{FE}} \leq \frac{1}{am} \cdot \frac{1}{\max_j (u_x)_j^2}, \quad a := \sum_{p=-m}^m \alpha_p^2,$$

where α_p are the coefficients in (9) and $(u_x)_j$ are given by (11). It is shown in Cheng, Kurganov, Qu, and Tang [2015] that

$$(19) \quad \|u(t + \Delta t_{\text{FE}})\|_{L^2} \leq \|u(t)\|_{L^2},$$

where $\|u(t)\|_{L^2} := \sqrt{\sum_j u_j^2(t) \Delta x}$.

Similar theoretical results hold for (13)–(15) with the forward Euler method, and for (16)–(17) with the forward Euler method. Note that the code DUMKA3 automatically selects time-steps so that in average the selected time-steps Δt_{ODE} are much larger than Δt_{FE} .

4.3 Pseudo-Spectral Methods for (2).

We first consider the 1-D equation,

$$(20) \quad u_t = -u_{xx} - \delta u_{xxxx}, \quad x \in [0, L], \quad t \in (0, T],$$

subject to the L -periodic boundary conditions.

We first use the FFT algorithm to compute the discrete Fourier coefficients $\{\widehat{u}_m(t)\}$ from the available point values $\{u_j(t)\}$. This gives us the following spectral approximation of u on $[0, L]$:

$$(21) \quad u(x, t) \approx \sum_m \widehat{u}_m(t) e^{i \frac{2\pi m x}{L}}.$$

We then substitute (21) into (20) and obtain very simple linear ODEs for the discrete Fourier coefficients of u ,

$$\frac{d}{dt} \widehat{u}_m(t) = (s - \delta s^2) \widehat{u}_m(t), \quad s = \left(\frac{2\pi m}{L}\right)^2,$$

which can be solved exactly:

$$\widehat{u}_m(t + \Delta t) = e^{(s - \delta s^2) \Delta t} \widehat{u}_m(t).$$

Finally, we use the inverse FFT algorithm to obtain the point values of the solution at the new time level, $\{u_j(t + \Delta t)\}$, out of the set of the discrete Fourier coefficients $\{\widehat{u}_m(t + \Delta t)\}$.

We now consider the 2-D equation (2),

$$u_t = -(u_{xx} + u_{yy}) - \delta(u_{xxxx} + 2u_{xxyy} + u_{yyyy}),$$

on a rectangular domain $\Omega = [0, L_x] \times [0, L_y]$ with the L_x - and L_y -periodic boundary conditions in the x - and y -directions, respectively.

Similar to the 1-D case, we apply the FFT algorithm and obtain very simple linear ODEs for the discrete Fourier coefficients of u ,

$$(22) \quad \frac{d}{dt} \widehat{u}_{m,\ell}(t) = (s - \delta s^2) \widehat{u}_{m,\ell}(t), \quad s = \left(\frac{2\pi m}{L_x}\right)^2 + \left(\frac{2\pi \ell}{L_y}\right)^2.$$

The exact solution of (22) is

$$\widehat{u}_{m,\ell}(t + \Delta t) = e^{(s - \delta s^2)\Delta t} \widehat{u}_{m,\ell}(t).$$

Finally, we apply the inverse FFT algorithm to obtain the point values of the solution at the new time level, $\{u_{j,k}(t + \Delta t)\}$, out of the set of the discrete Fourier coefficients $\{\widehat{u}_{m,\ell}(t + \Delta t)\}$.

As a numerical example, we again consider [Example 3.1](#) and compute its solution on a 128×128 uniform grid with the constant splitting step $\Delta t = 10^{-3}$. The solution computed at times $t = 1, 2, 5$ and 20 is shown in [Figure 7](#). These results are in good agreement with those reported in [Feng, Tang, and J. Yang \[2015\]](#) and with the SDC result reported in the last section.

We mention that the present operator-splitting approach can be combined with some time-adaptor strategy to speed up numerical simulations, see, e.g., [Cheng, Kurganov, Qu, and Tang \[2015\]](#), [Luo, Tang, and Xie \[2016\]](#), and [Qiao, Z. Zhang, and Tang \[2011\]](#).

We close this section by mentioning that some theoretical study for the operator splitting method outlined above was carried out in [X. Li, Qiao, and H. Zhang \[2017\]](#), where the finite difference scheme for the nonlinear part was improved so that larger time steps are allowed.

5 Concluding remarks

There have been considerable recent interests in developing highly stable and efficient numerical schemes for solving phase-field models. In this article, we present three classes of effective time discretization schemes. The first one is based on adding consistent terms so that the energy-decay property is satisfied. Some recent theory for this class of methods is reviewed. The second class is based on the time direction p -adaptivity, by combining lower-order convex-splitting methods and the SDC technique. It is demonstrated by numerical experiments that this is a very efficient numerical approach. The third class method is based on the classical operator-splitting method. Some preliminary results show that this is a promising method for practical computations.

References

- Assyr Abdulle (2002). “Fourth order Chebyshev methods with recurrence relation”. *SIAM J. Sci. Comput.* 23.6, pp. 2041–2054. MR: [1923724](#) (cit. on pp. [3666](#), [3669](#)).
- Andrea L. Bertozzi, Selim Esedoǰlu, and Alan Gillette (2007). “Inpainting of binary images using the Cahn-Hilliard equation”. *IEEE Trans. Image Process.* 16.1, pp. 285–291. MR: [2460167](#).
- Andrea L. Bertozzi, Ning Ju, and Hsiang-Wei Lu (2011). “A biharmonic-modified forward time stepping method for fourth order nonlinear diffusion equations”. *Discrete Contin. Dyn. Syst.* 29.4, pp. 1367–1391. MR: [2773188](#) (cit. on p. [3657](#)).
- Yuanzhen Cheng, Alexander Kurganov, Zhuolin Qu, and Tao Tang (2015). “Fast and stable explicit operator splitting methods for phase-field models”. *J. Comput. Phys.* 303, pp. 45–65. MR: [3422699](#) (cit. on pp. [3667](#), [3668](#), [3670](#), [3671](#)).
- Alina Chertock, Alexander Kurganov, and Guergana Petrova (2009). “Fast explicit operator splitting method for convection-diffusion equations”. *Internat. J. Numer. Methods Fluids* 59.3, pp. 309–332. MR: [2484270](#) (cit. on p. [3665](#)).
- Alok Dutt, Leslie Greengard, and Vladimir Rokhlin (2000). “Spectral deferred correction methods for ordinary differential equations”. *BIT* 40.2, pp. 241–266. MR: [1765736](#) (cit. on pp. [3659](#), [3664](#)).
- David J. Eyre (1993). “Systems of Cahn-Hilliard equations”. *SIAM J. Appl. Math.* 53.6, pp. 1686–1712. MR: [1247174](#) (cit. on pp. [3655](#), [3662](#)).
- Xinlong Feng, Tao Tang, and Jiang Yang (2013). “Stabilized Crank-Nicolson/Adams-Bashforth schemes for phase field models”. *East Asian J. Appl. Math.* 3.1, pp. 59–80. MR: [3109557](#) (cit. on p. [3655](#)).
- (2015). “Long time numerical simulations for phase-field problems using p -adaptive spectral deferred correction methods”. *SIAM J. Sci. Comput.* 37.1, A271–A294. MR: [3304267](#) (cit. on pp. [3655](#), [3661](#), [3662](#), [3664](#), [3671](#)).
- Hector Gomez and Thomas J. R. Hughes (2011). “Provably unconditionally stable, second-order time-accurate, mixed variational methods for phase-field models”. *J. Comput. Phys.* 230.13, pp. 5310–5327. MR: [2799512](#) (cit. on p. [3655](#)).
- Ruihan Guo, Yinhua Xia, and Yan Xu (2017). “Semi-implicit spectral deferred correction methods for highly nonlinear partial differential equations”. *J. Comput. Phys.* 338, pp. 269–284. MR: [3628250](#) (cit. on p. [3661](#)).
- Ruihan Guo and Yan Xu (2016). “Local discontinuous Galerkin method and high order semi-implicit scheme for the phase field crystal equation”. *SIAM J. Sci. Comput.* 38.1, A105–A127. MR: [3439767](#) (cit. on pp. [3661](#), [3664](#)).
- Yinnian He, Yunxian Liu, and Tao Tang (2007). “On large time-stepping methods for the Cahn-Hilliard equation”. *Appl. Numer. Math.* 57.5-7, pp. 616–628. MR: [2322435](#) (cit. on pp. [3655](#)–[3657](#)).

- R. V. Kohn (2006). “Energy-driven pattern formation”. In: *Proceedings of the International Congress of Mathematicians, Madrid, 2006*. European Math. Soc., pp. 359–383 (cit. on p. 3654).
- J. Shen L.Q. Chen (1998). “Applications of semi-implicit Fourier-spectral method to phase field equations”. *Comput. Phys. Comm.* 108, pp. 147–158 (cit. on p. 3655).
- Dong Li and Zhonghua Qiao (2017a). “On second order semi-implicit Fourier spectral methods for 2D Cahn-Hilliard equations”. *J. Sci. Comput.* 70.1, pp. 301–341. MR: 3592143 (cit. on p. 3659).
- (2017b). “On the stabilization size of semi-implicit Fourier-spectral methods for 3D Cahn-Hilliard equations”. *Commun. Math. Sci.* 15.6, pp. 1489–1506. MR: 3668944 (cit. on p. 3659).
- Dong Li, Zhonghua Qiao, and Tao Tang (2016). “Characterizing the stabilization size for semi-implicit Fourier-spectral method to phase field equations”. *SIAM J. Numer. Anal.* 54.3, pp. 1653–1681. MR: 3507555 (cit. on pp. 3657, 3659).
- Xiao Li, Zhonghua Qiao, and Hui Zhang (2017). “Convergence of a fast explicit operator splitting method for the epitaxial growth model with slope selection”. *SIAM J. Numer. Anal.* 55.1, pp. 265–285. MR: 3608748 (cit. on p. 3671).
- Fuesheng Luo, Tao Tang, and Hehu Xie (2016). “Parameter-free time adaptivity based on energy evolution for the Cahn-Hilliard equation”. *Commun. Comput. Phys.* 19.5, pp. 1542–1563. MR: 3501222 (cit. on p. 3671).
- A. A. Medovikov (n.d.). “DUMKA3 code” (cit. on p. 3669).
- Alexei A. Medovikov (1998). “High order explicit methods for parabolic equations”. *BIT* 38.2, pp. 372–390. MR: 1638136 (cit. on p. 3669).
- Michael L. Minion (2003). “Semi-implicit spectral deferred correction methods for ordinary differential equations”. *Commun. Math. Sci.* 1.3, pp. 471–500. MR: 2069941 (cit. on p. 3664).
- Zhonghua Qiao and Shuyu Sun (2014). “Two-phase fluid simulation using a diffuse interface model with Peng-Robinson equation of state”. *SIAM J. Sci. Comput.* 36.4, B708–B728. MR: 3246906 (cit. on p. 3655).
- Zhonghua Qiao, Zhi-Zhong Sun, and Zhengru Zhang (2015). “Stability and convergence of second-order schemes for the nonlinear epitaxial growth model without slope selection”. *Math. Comp.* 84.292, pp. 653–674. MR: 3290959 (cit. on p. 3655).
- Zhonghua Qiao, Zhengru Zhang, and Tao Tang (2011). “An adaptive time-stepping strategy for the molecular beam epitaxy models”. *SIAM J. Sci. Comput.* 33.3, pp. 1395–1414. MR: 2813245 (cit. on pp. 3658, 3671).
- J. Shen, J. Xu, and J. Yang (2017). “A new class of efficient and robust energy stable schemes for gradient flows” (cit. on pp. 3655, 3662).

- Jie Shen, Tao Tang, and Li-Lian Wang (2011). *Spectral methods*. Vol. 41. Springer Series in Computational Mathematics. Algorithms, analysis and applications. Springer, Heidelberg, pp. xvi+470. MR: [2867779](#) (cit. on p. [3663](#)).
- Jie Shen, Cheng Wang, Xiaoming Wang, and Steven M. Wise (2012). “Second-order convex splitting schemes for gradient flows with Ehrlich-Schwoebel type energy: application to thin film epitaxy”. *SIAM J. Numer. Anal.* 50.1, pp. 105–125. MR: [2888306](#) (cit. on pp. [3655](#), [3662](#)).
- Jie Shen and Xiaofeng Yang (2010). “Numerical approximations of Allen-Cahn and Cahn-Hilliard equations”. *Discrete Contin. Dyn. Syst.* 28.4, pp. 1669–1691. MR: [2679727](#) (cit. on pp. [3655](#), [3656](#)).
- Huailing Song and Chi-Wang Shu (2017). “Unconditional energy stability analysis of a second order implicit-explicit local discontinuous Galerkin method for the Cahn-Hilliard equation”. *J. Sci. Comput.* 73.2-3, pp. 1178–1203. MR: [3719623](#) (cit. on p. [3659](#)).
- Tao Tang, Hehu Xie, and Xiaobo Yin (2013). “High-order convergence of spectral deferred correction methods on general quadrature nodes”. *J. Sci. Comput.* 56.1, pp. 1–13. MR: [3049939](#) (cit. on p. [3664](#)).
- J. G. Verwer, B. P. Sommeijer, and W. Hundsdorfer (2004). “RKC time-stepping for advection-diffusion-reaction problems”. *J. Comput. Phys.* 201.1, pp. 61–79. MR: [2098853](#) (cit. on p. [3669](#)).
- S. M. Wise, C. Wang, and J. S. Lowengrub (2009). “An energy-stable and convergent finite-difference scheme for the phase field crystal equation”. *SIAM J. Numer. Anal.* 47.3, pp. 2269–2288. MR: [2519603](#) (cit. on p. [3655](#)).
- Yinhua Xia, Yan Xu, and Chi-Wang Shu (2009). “Application of the local discontinuous Galerkin method for the Allen-Cahn/Cahn-Hilliard system”. *Commun. Comput. Phys.* 5.2-4, pp. 821–835. MR: [2513717](#) (cit. on p. [3655](#)).
- Chuanju Xu and Tao Tang (2006). “Stability analysis of large time-stepping methods for epitaxial growth models”. *SIAM J. Numer. Anal.* 44.4, pp. 1759–1779. MR: [2257126](#) (cit. on pp. [3655](#), [3657](#), [3658](#)).
- Kristoffer G. van der Zee, J. Tinsley Oden, Serge Prudhomme, and Andrea Hawkins-Daarud (2011). “Goal-oriented error estimation for Cahn-Hilliard models of binary phase transition”. *Numer. Methods Partial Differential Equations* 27.1, pp. 160–196. MR: [2743604](#) (cit. on p. [3655](#)).
- J. Zhu, L.-Q. Chen, J. Shen, and V. Tikare (1999). “Coarsening kinetics from a variable-mobility Cahn-Hilliard equation: Application of a semi-implicit Fourier spectral method”. *Phys. Rev. E* 60, pp. 3564–3572 (cit. on pp. [3655](#)–[3657](#)).

Received 2018-02-26.

Department of Mathematics, Southern University of Science and Technology, Nanshan District, Shenzhen,
Guangdong 518055, China
tangt@sustc.edu.cn

For ICM 2018 participants only

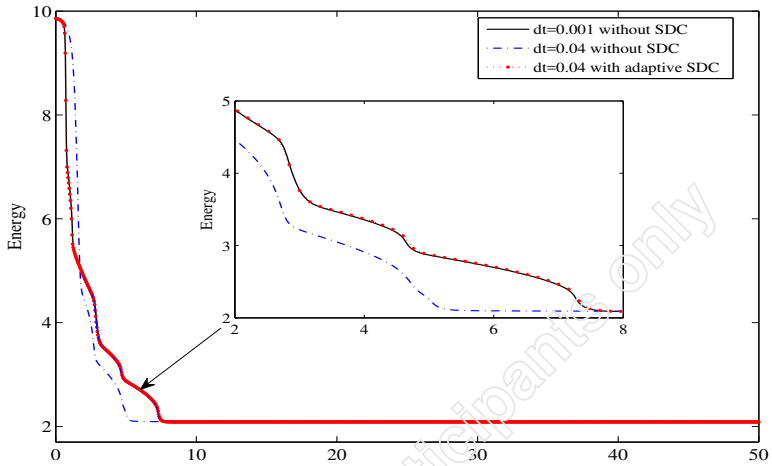


Figure 4: [Example 3.1](#): Energy curves of the Cahn-Hilliard equation by different schemes with different time steps.

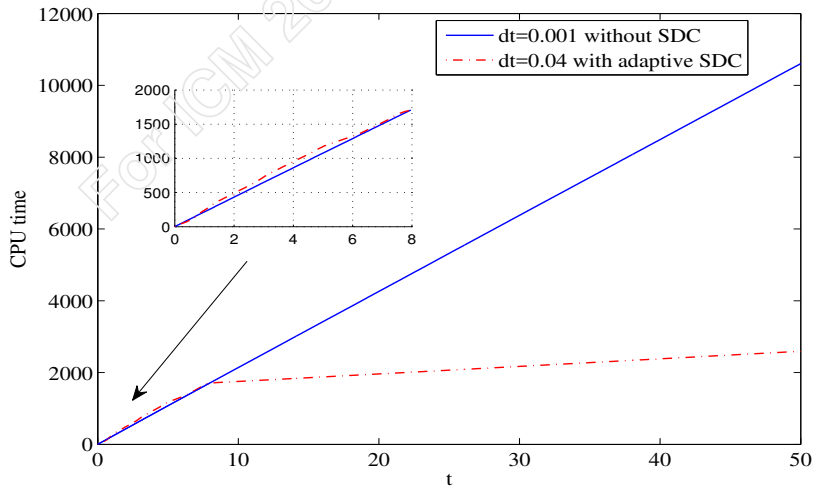


Figure 5: [Example 3.1](#): CPU time comparison between different schemes for Cahn-Hilliard equation.

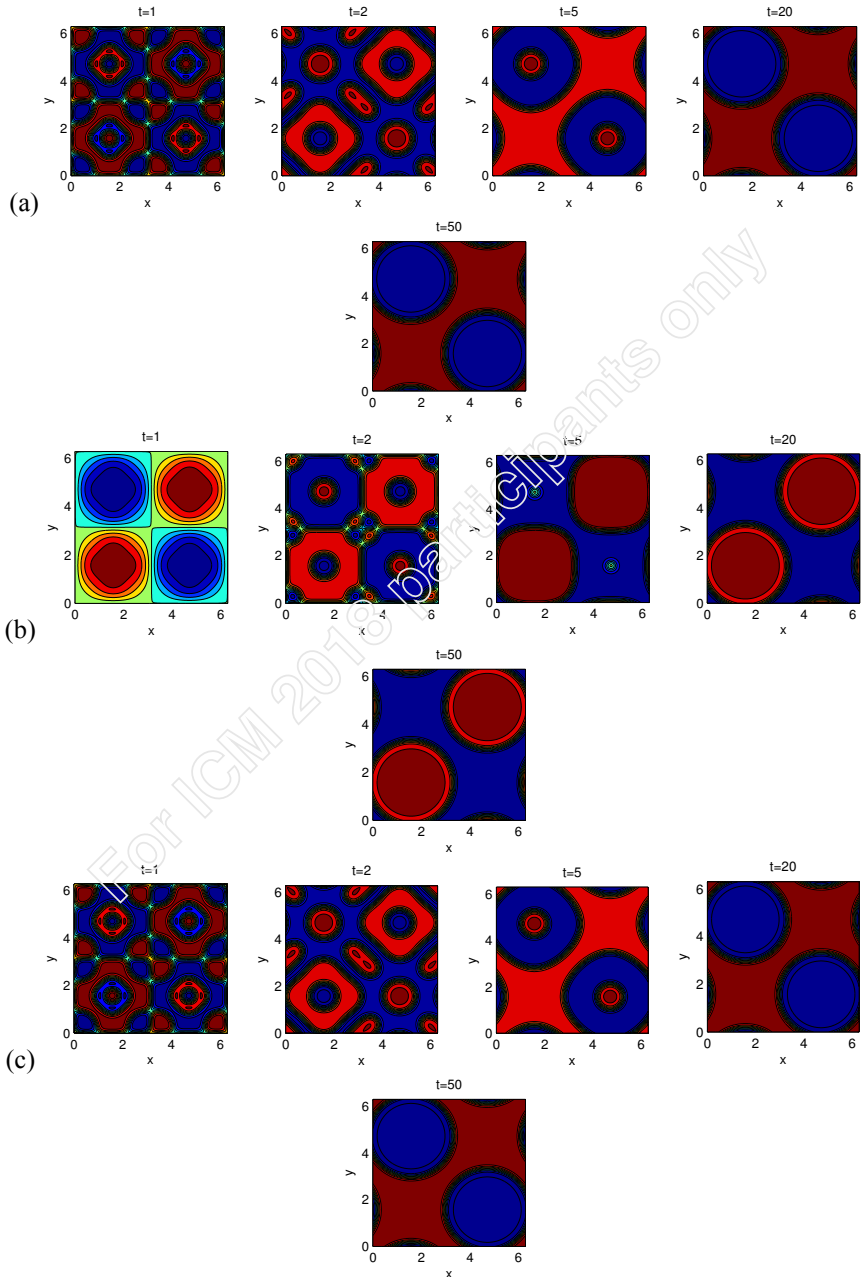


Figure 6: [Example 3.1](#): Solution variation at different time, using (a) direct energy

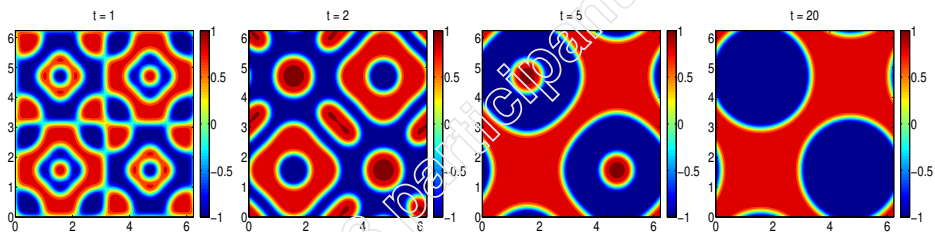


Figure 7: [Example 3.1](#): u computed with splitting time-stepping with $\Delta t = 10^{-3}$.